

CtrTab: Tabular Data Synthesis with High-Dimensional and Limited Data

Zuqing Li, Jianzhong Qi, Junhao Gan

The University of Melbourne

zuqingl@student.unimelb.edu.au,
{jianzhong.qi, junhao.gan}@unimelb.edu.au,

Abstract

Diffusion-based tabular data synthesis models have yielded promising results. However, we observe that when the data dimensionality increases, existing models tend to degenerate and may perform even worse than simpler, non-diffusion-based models. This is because limited training samples in high-dimensional space often hinder generative models from capturing the distribution accurately. To address this issue, we propose CtrTab – a condition controlled diffusion model for tabular data synthesis – to improve the performance of diffusion-based generative models in high-dimensional, low-data scenarios. Through CtrTab, we inject samples with added Laplace noise as control signals to improve data diversity and show its resemblance to L_2 regularization, which enhances model robustness. Experimental results across multiple datasets show that CtrTab outperforms state-of-the-art models, with performance gap in accuracy over 80% on average. Our source code will be released upon paper publication.

1 Introduction

Tabular data synthesis is an important problem with wide range of applications. For example, in fields such as healthcare and finance, real-world data often contain sensitive information that cannot be directly shared for privacy considerations. It is crucial to generate synthetic data which not only closely resembles real data, but also avoids exposing sensitive information [Kotelnikov *et al.*, 2023]. In machine learning applications, data augmentation is done to enrich the data (which often takes a tabular form) for model training, especially for class imbalanced datasets. Model training with both real and synthetic data often improves machine learning performance compared to training with real data alone.

Early studies on tabular data synthesis are primarily based on statistical models [Aggarwal and Yu, 2004; Barak *et al.*, 2007; Park *et al.*, 2013; Li *et al.*, 2014; Zhang *et al.*, 2014]. With the rise of deep learning, models based on GANs and diffusion [Chen *et al.*, 2019; Xu *et al.*, 2019; Kim *et al.*, 2021; Kotelnikov *et al.*, 2023; Liu *et al.*, 2024] have been widely applied to the task. At the same time, in order to ensure the

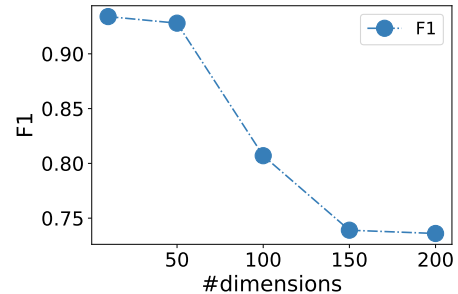


Figure 1: Challenges in tabular data synthesis over high-dimensional data. On a dataset generated using the *sklearn* package, as the dimensionality increases, the performance (F1 score) of the state-of-the-art diffusion-based model TabSyn [Zhang *et al.*, 2024] in machine learning tests decreases (detailed in Section 6.2).

quality of generated data, some studies have introduced conditional generation models [Xu *et al.*, 2019; Zhao *et al.*, 2023; Liu *et al.*, 2024], aiming to incorporate additional information to guide the table synthesis process.

However, an issue that has been missed by the existing studies is the challenges brought by sparse, high-dimensional tabular data (i.e., tables with many columns and only a few rows). For example, in the field of biomedicine, data often have very high dimensionality, while the sample size is relatively small due to the high sampling costs. This phenomenon is known as the notorious curse of dimensionality.

Specifically, data in high-dimensional spaces tends to be sparse, and the limited amount of training data makes it difficult to learn the true distribution. Even the performance of the state-of-the-art diffusion model [Zhang *et al.*, 2024] for tabular data synthesis is still far from satisfactory on this task, as shown in Figure 1. Having a large number of features with a limited number of training samples, machine learning models may struggle to adequately learn across all the dimensions.

To address this issue, we propose a condition controlled diffusion model for tabular data synthesis named **CtrTab**. Building upon the classifier-free guidance Denoising Diffusion Probabilistic Model (CFG DDPM) [Ho and Salimans, 2021; Zhang *et al.*, 2023], we introduce a control module in CtrTab besides a denoising network. The control module takes an additional input, a condition C_f , which is encoded through a neural network and then fed back into the decoder

of the denoising network.

Traditional diffusion models focus on unconditional implicit generation, which may lead to unstable or deviated results on high-dimensional data [Bao *et al.*, 2022]. In contrast, our control module is explicit and incorporates clear conditional control signals directly into the denoising network. This way, our control module effectively enhances the controllability and reduces the inefficiency of the model’s random exploration in the high-dimensional space.

We further use a noise injection training method to improve the diversity of the training data. Specifically, we add Laplace noise to the training samples, which is known to be effective to protect data privacy. Moreover, we theoretically show that the noise injection training is effectively an L_2 regularization, which helps CtrTab’s generalization capability.

Through extensive experiments, we show that although other designs, such as perturbing the data with noise to populate the training set size or introducing more parameters to existing models, can also improve model performance, these designs still have limitations while their performance suboptimal. This underscores the challenge for diffusion models in learning complex distributions in high-dimensional spaces and the advantages of our model design.

Our contributions are summarized as follows:

1. We propose a diffusion-based tabular data synthesis model named CtrTab to address challenges brought by sparse, high-dimensional data. CtrTab comes with a control module and a noise injection training method. These effectively enhance the generative performance of CtrTab on high-dimensional tabular data.
2. We theoretically show that our noise-based training is analogous to an L_2 regularization, where the noise scale controls the regularization strength, offering a flexible trade-off in generation.
3. We conduct extensive experiments to verify the effectiveness of CtrTab over real datasets. The results show that machine learning models trained with data synthesized by CtrTab is much more accurate than those trained with data synthesized by existing models including the SOTA, with a performance gain of over 80% on average, confirming that CtrTab is more effective in learning the data distribution.

2 Related Work

Tabular Data Synthesis Early studies [Aggarwal and Yu, 2004; Barak *et al.*, 2007; Li *et al.*, 2014; Park *et al.*, 2013; Zhang *et al.*, 2014] mainly use statistical models for tabular data synthesis. The synthesized data distribution often deviates much from that of the original data, leading to suboptimal performance in downstream tasks such as low accuracy for the machine learning models trained with the synthesized data [Xu *et al.*, 2019]. In the era of deep learning, *Generative Adversarial Networks* (GANs)-based models have become popular for the task [Park *et al.*, 2018; Chen *et al.*, 2019; Xu *et al.*, 2019; Kim *et al.*, 2021; Wen *et al.*, 2022; Zhao *et al.*, 2023]. Due to the instability of GAN training [Arjovsky *et al.*, 2017], alternative models are explored, with diffusion-based models being a promising choice [Kim *et al.*, 2023;

Kotelnikov *et al.*, 2023; Lee *et al.*, 2023; Liu *et al.*, 2024; Shi *et al.*, 2024; Zhang *et al.*, 2024]. Our model represents a latest development of the diffusion-based models.

Conditional Tabular Data Synthesis Conditional generative models have been proposed to for tabular data synthesis with additional constraints. For example, CTGAN [Xu *et al.*, 2019] introduces class label information into the GAN generator to generate data corresponding to the given classes. CTAB-GAN+ [Zhao *et al.*, 2023] extends the CTGAN model to support both discrete and continuous data class labels. RelDDPM [Liu *et al.*, 2024] uses a classifier-guided *conditional diffusion model*. They start with training an unconditional diffusion model to fit the input data distribution. Then, given a constraint, e.g., a target class label, they train a classifier and use the gradient information from this classifier to control sample generation. Unlike these models, our model does not concern generating data for a particular class but uses a control module to add constraints and guide the model to fit a high-dimensional distribution with sparse data. There are also works utilizing LLMs [Fang *et al.*, 2024; Wang *et al.*, 2024]. We aim for lighter-weight solutions and do not consider such solutions further.

Learning High-Dimensional Distribution with Sparse Data High-dimensional data poses significant challenges for machine learning. In *probably approximately correct* (PAC) learning [Valiant, 1984], the generalization error of a model depends on both the data dimensionality and the hypothesis class complexity. Typically, both the hypothesis space complexity and the required sample size grow exponentially as the dimensionality increases, making generalization more difficult. For generative models, the increased dimensionality results in sparse data distributions [Bishop, 2006], making it difficult for models to capture the underlying data structure. In other fields, such as computer vision, common solutions to address the data sparsity issue with high-dimensional data use data augmentation techniques, such as rotating and cropping images to generate more samples, as well as feature extraction and dimensionality reduction [Shorten and Khoshgoftaar, 2019]. Our study addresses this issue in the context of tabular data synthesis.

3 Preliminaries

Problem Statement Consider a table \mathcal{T} of N rows, where each row consists of D_{num} numerical features and D_{cat} categorical features that correspond to variables \mathbf{x}_{num} and \mathbf{x}_{cat} , respectively. Typically, categorical variables need to be encoded with some numerical representations (e.g., one-hot encoding) before serving as model input. Let the dimensionality of the all categorical variables after the encoding be $E(D_{\text{cat}})$. The total model input data dimensionality is then $D = E(D_{\text{cat}}) + D_{\text{num}}$. Each row of \mathcal{T} , which is considered a data sample, is expressed as $\mathbf{x} = [\mathbf{x}_{\text{num}}, \mathbf{x}_{\text{cat}}]$, where $\mathbf{x}_{\text{num}} \in \mathbb{R}^{D_{\text{num}}}$ and $\mathbf{x}_{\text{cat}} \in \mathbb{R}^{E(D_{\text{cat}})}$.

The aim of this work, is to train a generative model $p_{\theta}(\mathcal{T})$ such that the distribution of the generated data approximates that of the real data (i.e., rows) in \mathcal{T} . Our focus is on sparse, high-dimensional data, where $N \ll 2^D$. Here, 2^D represents the volume of the data space, which grows exponentially with

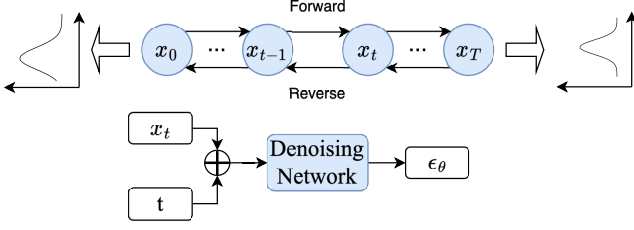


Figure 2: Denoising diffusion probabilistic model architecture

D. We design our model CtrTab based on diffusion models. Below, we brief the core idea of diffusion models. Readers who are familiar with such models can skip to Section 4.

Denoising Diffusion Probabilistic Model The denoising diffusion probabilistic model (DDPM) [Ho *et al.*, 2020] has two processes: a forward process and a reverse process, both of which are defined as Markov chains. The overall model structure is shown in Figure 2. In the **forward process**, noise is added to a data sample \mathbf{x}_0 from the distribution $q(\mathbf{x}_0)$:

$$q(\mathbf{x}_t|\mathbf{x}_{t-1}) = \mathcal{N}(\mathbf{x}_t; \sqrt{1 - \beta_t}\mathbf{x}_{t-1}, \beta_t\mathbf{I}), \quad (1)$$

$$q(\mathbf{x}_t|\mathbf{x}_0) = \mathcal{N}(\mathbf{x}_t; \sqrt{\bar{\alpha}_t}\mathbf{x}_0, (1 - \bar{\alpha}_t)\mathbf{I}), \quad (2)$$

where t is the number of noise adding steps (timesteps), β_t controls the variance of the noise, $\alpha_t = 1 - \beta_t$, and $\bar{\alpha}_t = \prod_{i=1}^t \alpha_i$.

In the **reverse process**, given a sample \mathbf{x}_t with pure random noise which is usually from a Gaussian distribution,

a *denoising network* (i.e., the diffusion model) learns to iteratively denoise \mathbf{x}_t until it is restored to the initial sample \mathbf{x}_0 . The reverse process can also be expressed as a Gaussian distribution through derivation:

$$q(\mathbf{x}_{t-1}|\mathbf{x}_t, \mathbf{x}_0) = \mathcal{N}(\mathbf{x}_{t-1}; \tilde{\mu}_t(\mathbf{x}_t, \mathbf{x}_0), \tilde{\beta}_t), \quad (3)$$

where $\tilde{\mu}_t(\mathbf{x}_t, \mathbf{x}_0) = \frac{\sqrt{\bar{\alpha}_{t-1}\beta_t}}{1 - \bar{\alpha}_t}\mathbf{x}_0 + \frac{\sqrt{\bar{\alpha}_t(1 - \bar{\alpha}_{t-1})}}{1 - \bar{\alpha}_t}\mathbf{x}_t$ and $\tilde{\beta}_t = \frac{1 - \bar{\alpha}_{t-1}}{1 - \bar{\alpha}_t}\beta_t$.

The model learning process aims to maximize the variational lower bound:

$$\log(q(\mathbf{x})) \geq E_q \left[\underbrace{\log p_\theta(\mathbf{x}_0|\mathbf{x}_1)}_{L_0} - \underbrace{D_{KL}(q(\mathbf{x}_T|\mathbf{x}_0)||p(\mathbf{x}_T))}_{L_T} - \sum_{t>1} \underbrace{D_{KL}(q(\mathbf{x}_{t-1}|\mathbf{x}_t, \mathbf{x}_0)||p_\theta(\mathbf{x}_{t-1}|\mathbf{x}_t))}_{L_{t-1}} \right], \quad (4)$$

where $D_{KL}(\cdot)$ denotes the KL divergence, $q(\mathbf{x})$ denotes the probability distribution of \mathbf{x}_0 , p_θ denotes the parameterized model θ used to approximate the probability distribution of the reverse process, and T represents the timestep at which noise is added, such that the distribution of the original data matches the standard Gaussian distribution. To maximize this lower bound means to minimize the KL divergence between $q(\mathbf{x}_{t-1}|\mathbf{x}_t, \mathbf{x}_0)$ and $p_\theta(\mathbf{x}_{t-1}|\mathbf{x}_t)$.

With further simplifications, the objective reduces to minimizing the sum of mean-squared errors between ϵ and ϵ_θ , where ϵ is the ground truth error from \mathbf{x}_0 to \mathbf{x}_t and ϵ_θ is the predicted noise by a denoising network:

$$L_{\text{simple}}(\theta) = \mathbb{E}_{\mathbf{x}_0, t, \epsilon} [\|\epsilon - \epsilon_\theta(\mathbf{x}_t, t)\|^2], \quad (5)$$

Here, t and ϵ are generated randomly during training, while \mathbf{x}_t is obtained by adding noise to \mathbf{x}_0 with Equation (2).

Once trained, the denoising network ϵ_θ is used for data generation (called the sampling process). It takes \mathbf{x}_t and a timestep t as input, and its goal is to denoise \mathbf{x}_t iteratively back to \mathbf{x}_0 (i.e., a generated sample). Specifically, at each timestep t , it computes \mathbf{x}_{t-1} from \mathbf{x}_t as follows:

$$\mathbf{x}_{t-1} = \frac{1}{\sqrt{\alpha_t}} \left(\mathbf{x}_t - \frac{1 - \alpha_t}{\sqrt{1 - \bar{\alpha}_t}} \epsilon_\theta(\mathbf{x}_t, t) \right) + \sigma_t \mathbf{z}, \quad (6)$$

where σ_t is the *noise scale* at timestep t , and \mathbf{z} follows the standard Gaussian distribution.

Score-based Diffusion Generative Model The initial proposal of diffusion models use discrete timesteps as described above. *Score-based generative models* [Song *et al.*, 2021] further introduce a continuous-time formulation using Stochastic Differential Equations (SDEs), where the forward and reverse processes are guided by a *score function* $\nabla_{\mathbf{x}} \log p_t(\mathbf{x})$. Score-based SDE is defined with the following forward and backward equations:

$$\begin{aligned} d\mathbf{x} &= \mathbf{f}(\mathbf{x}, t)dt + g(t) d\mathbf{w}_t, \\ d\mathbf{x} &= [\mathbf{f}(\mathbf{x}, t) - g^2(t)\nabla_{\mathbf{x}} \log p_t(\mathbf{x})]dt + g(t)d\mathbf{w}_t, \end{aligned} \quad (7)$$

where \mathbf{f} and g are the drift and diffusion coefficients, and the diffusion process is typically divided into variance preserving (VP) and variance exploding (VE), and \mathbf{w} is the standard Wiener process. Our solution supports the VE diffusion process, the training objective of which is to minimize the following equation [Zhang *et al.*, 2024]:

$$\begin{aligned} L(\theta) &= \mathbb{E}_{\mathbf{x}_0} \mathbb{E}_{\mathbf{x}_t|\mathbf{x}_0} \|D_\theta(\mathbf{x}_t, t) - \nabla_{\mathbf{x}_t} \log p(\mathbf{x}_t|\mathbf{x}_0)\|^2 \\ &\approx \mathbb{E}_{\mathbf{x}_0} \mathbb{E}_{\mathbf{x}_t|\mathbf{x}_0} \|\epsilon_\theta(\mathbf{x}_t, t) - \epsilon\|_2^2. \end{aligned} \quad (8)$$

Like DDPM, the denoising network here is trained to predict the noise at timestep t . Our model thus is designed to support both DDPM and score-based SDE, upon which existing diffusion-based tabular data synthesis models are built. For simplicity, we use diffusion model to refer to both types of models hereafter when the context is clear.

4 Methodology

This section presents our CtrTab model, which incorporates a control module that can be applied to diffusion-based tabular data synthesis models. By incorporating the control module, CtrTab is trained on noisy data in addition to raw input data \mathcal{T} to learn the input distribution more effectively, as will be shown by our theoretical analysis in Section 5.

Inspired by a recent model [Zhang *et al.*, 2023] proposed for text-to-image generation, our CtrTab model takes a two branches – a denoising network based on some diffusion model, and a control module, as illustrated in Figure 3.

Denoising Network The denoising network takes a noisy sample \mathbf{x}_t (which comes from a ground truth sample \mathbf{x}_0 during training and from standard Gaussian noise during sampling) and a timestep t as input, and it outputs a predicted noise ϵ_θ . Specifically, it uses an autoencoder, consisting of a symmetrical encoder and decoder. For the hidden layers, we follow the state-of-the-art (SOTA) model TabSyn (which is based on score-based SDE) [Zhang *et al.*, 2024], where each

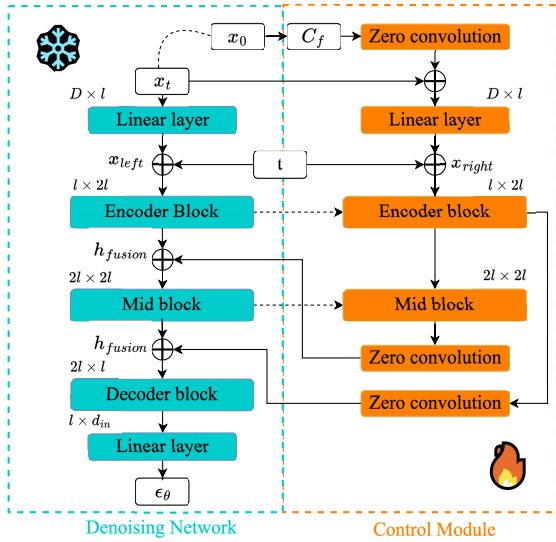


Figure 3: CtrTab model architecture.

block consists of a linear layer and a SiLU activation function. We omit the detailed steps for conciseness. Note that the hidden layers can also follow those of DDPM straightforwardly.

Control Module The control module takes a condition C_f as an additional input. In our model, C_f is set to be the ground truth sample x_0 added with a noise. The goal is to perform conditional generation. This design is analogous to classifier-free guidance [Zhang *et al.*, 2023], where the condition is directly incorporated into the diffusion model during training to instruct the generation of samples that satisfy the condition.

Noisy input. We use Laplace noise to form C_f for its empirical effectiveness (see Section 6.2) and that it is often used to help protect data privacy [Dwork and Roth, 2014], which is a common application of tabular data synthesis (we leave how this design helps protect data privacy for future work as it is beyond the scope of this study).

Thus, we set:

$$C_f = x_0 + \text{Laplace}(b), \quad (9)$$

where $\text{Laplace}(b)$ represents the Laplace noise with mean 0 and variance $2b^2 - b$ is the *noise scale* factor.

The control module and the denoising network interact in two fusion steps: *input fusion* and *control fusion*.

Input fusion. Both the control module and the denoising network share the input x_t and t . They share the same sinusoidal timestep embedding t_{emb} [Kotelnikov *et al.*, 2023; Liu *et al.*, 2024; Zhang *et al.*, 2024]:

$$t_{\text{emb}} = \text{Linear}(\text{SiLU}(\text{Linear}(\text{SinTimeEmb}(t))))), \quad (10)$$

The timestep embedding is fused with x_t for the two modules, which yields:

$$\begin{aligned} x_{\text{left}} &= \text{Linear}(x_t) + t_{\text{emb}}, \\ x_{\text{right}} &= \text{Linear}(\text{zero_convolution}(C_f) + x_t) + t_{\text{emb}}. \end{aligned} \quad (11)$$

Here, x_{left} represents the output of the top linear layer of the denoising network, and x_{right} represents the output of the

top *zero convolution* and linear layers (see Figure 3). The zero convolution layer is a convolutional layer with 1×1 kernel size, where the weight and bias are initialized to 0. The purpose is to learn effective encoded information of the condition through zero convolution layers and linear layers, before incorporating it into the decoding layers of the denoising network to guide the output.

Control fusion. The embedding x_{right} then goes through an encoder block and a mid block, which are copied from the denoising network. Note that we train denoising network beforehand, and it is frozen when the control module is trained, to retain the strong data synthesis capability of the denoising network for denser, low dimensional data.

Let h_{left} be the hidden outputs of the encoder block and the mid blocks of the denoising network. Let h_{right} be the output of the counterpart blocks on the control module. These outputs are fused as:

$$h_{\text{fusion}} = h_{\text{left}} + \text{zero_convolution}(h_{\text{right}}). \quad (12)$$

Training and Inference The training objectives of CtrTab using DDPM and score-based SDE as the denoising network are to minimize the following equations, respectively:

$$\begin{aligned} L_{DDPM}(\theta) &= \mathbb{E}_{x_0, t, \epsilon, C_f} \|\epsilon - \epsilon_\theta(x_t, t, C_f)\|^2, \\ L_{SDE}(\theta) &= \mathbb{E}_{x_0} \mathbb{E}_{x_t | x_0} \mathbb{E}_{C_f} \|\epsilon - \epsilon_\theta(x_t, t, C_f)\|^2. \end{aligned} \quad (13)$$

As mentioned above, when the control module is trained, while the forward and backward propagation process go through the denoising network, only the parameters of the control module are updated.

Algorithm 1 and 2 summarize the training and the inference (i.e., sampling) processes of CtrTab, respectively.

Algorithm 1 Training

for each step do
 Sample $x_0 \sim q(x_0)$
 Sample t, ϵ
 Get perturbed data x_t and C_f
 Calculate loss $\|\epsilon - \epsilon_\theta(x_t, C_f, t)\|^2$
 Update the the control module via backpropagation
end for
return Trained CtrTab

Algorithm 2 Sampling

Sample x_T, C_f
for $t = T, \dots, 1$ **do**
 Predict $\epsilon_\theta(x_t, C_f, t)$ using the CtrTab outputs
 Obtain x_{t-1} through the reverse equation of CtrTab
end for
return x_0

5 Theoretical Results

Next, we show that by adding appropriate noise, the training objective is analogous to an objective with an L_2 -regularization, which is known to be effective to controlling

the curve fitting of the true distribution [Ng, 2004]. Here, we present a summary of the theoretical results, while the detailed proof can be found in Appendix A.1 in the supplementary material (same below).

For simplicity, we prove this result based on the training objective derived from DDPM [Ho *et al.*, 2020]. The proof for the case with the training objective of score-based SDE is analogous and omitted for conciseness. Note here we denote \mathbf{C}_f as the condition without noise, and $\mathbf{C}_f + \tilde{\epsilon}$ as the noise added condition.

Theorem 1. *Let the training objective of CtrTab be minimizing $\mathcal{L} = \mathbb{E}_{\mathbf{x}_0, t, \epsilon, \mathbf{C}_f} \|\epsilon - \epsilon_\theta(\mathbf{x}_t, t, \mathbf{C}_f)\|^2$, and let the training objective with a noise added condition be minimizing $\tilde{\mathcal{L}} = \mathbb{E}_{\mathbf{x}_0, t, \epsilon, \mathbf{C}_f, \tilde{\epsilon}} \|\epsilon - \epsilon_\theta(\mathbf{x}_t, t, \mathbf{C}_f + \tilde{\epsilon})\|^2$, where $\tilde{\epsilon}$ is a noise drawn from a distribution with mean 0 and variance η^2 . Then, $\tilde{\mathcal{L}} = \mathcal{L} + \eta^2 \mathcal{L}^R$ holds, where \mathcal{L}^R is a regularization term in the Tikhonov form.*

Proof Sketch. Expansion of the training objectives. Following previous works [Bishop, 1995; Webb, 1994], we define $y(\mathbf{C}_f) = \epsilon_\theta(\mathbf{x}_t, t, \mathbf{C}_f)$ for simplicity. Then $\mathcal{L} = \mathbb{E}_{\mathbf{x}_0, t, \epsilon, \mathbf{C}_f} \|\epsilon - \epsilon_\theta(\mathbf{x}_t, t, \mathbf{C}_f)\|^2$ can be expanded as follows:

$$\mathcal{L} = \int \int \int \int \{y(\mathbf{C}_f) - \epsilon\}^2 p(\epsilon|t, \mathbf{x}_0, \mathbf{C}_f) p(t, \mathbf{x}_0, \mathbf{C}_f) dt d\mathbf{x}_0 d\epsilon d\mathbf{C}_f. \quad (14)$$

Also, $\tilde{\mathcal{L}} = \mathbb{E}_{\mathbf{x}_0, t, \epsilon, \mathbf{C}_f, \tilde{\epsilon}} \|\epsilon - \epsilon_\theta(\mathbf{x}_t, t, \mathbf{C}_f + \tilde{\epsilon})\|^2$ becomes:

$$\tilde{\mathcal{L}} = \int \int \int \int \int \{y(\mathbf{C}_f + \tilde{\epsilon}) - \epsilon\}^2 p(\epsilon|t, \mathbf{x}_0, \mathbf{C}_f) p(t, \mathbf{x}_0, \mathbf{C}_f) p(\tilde{\epsilon}) dt d\mathbf{x}_0 d\epsilon d\mathbf{C}_f d\tilde{\epsilon} \quad (15)$$

Some preliminaries. Expanding $y(\mathbf{C}_f + \tilde{\epsilon})$ with Taylor series, and assuming that the noise amplitude is small such that any term of order $O(\tilde{\epsilon}^3)$ or higher can be neglected, we have:

$$y(\mathbf{C}_f + \tilde{\epsilon}) = y(\mathbf{C}_f) + \sum_i \tilde{\epsilon}_i \left. \frac{\partial y}{\partial \mathbf{C}_{f,i}} \right|_{\tilde{\epsilon}=0} + \frac{1}{2} \sum_i \sum_j \tilde{\epsilon}_i \tilde{\epsilon}_j \left. \frac{\partial^2 y}{\partial \mathbf{C}_{f,i} \partial \mathbf{C}_{f,j}} \right|_{\tilde{\epsilon}=0} + O(\tilde{\epsilon}^3) \quad (16)$$

By the fact that $\tilde{\epsilon}$ is chosen from a distribution with mean 0 and variance η^2 , we have the following equalities:

$$\int \tilde{\epsilon}_i p(\tilde{\epsilon}) d\tilde{\epsilon} = 0, \quad \int \tilde{\epsilon}_i \tilde{\epsilon}_j p(\tilde{\epsilon}) d\tilde{\epsilon} = \eta^2 \delta_{ij}, \text{ where } \delta_{ij} = \begin{cases} 1 & i = j \\ 0 & i \neq j \end{cases}. \quad (17)$$

The training objective with noise is a regularization. By substituting Equation (16) into Equation (15), we obtain:

$$\tilde{\mathcal{L}} = \mathcal{L} + \eta^2 \mathcal{L}^R, \text{ where} \quad (18)$$

$$\mathcal{L}^R = \int \int \int \int \sum_i \left\{ \left(\frac{\partial y}{\partial \mathbf{C}_{f,i}} \right)^2 + (y(\mathbf{C}_f) - \epsilon) \frac{\partial^2 y}{\partial \mathbf{C}_{f,i}^2} \right\} p(\epsilon|t, \mathbf{x}_0, \mathbf{C}_f) p(t, \mathbf{x}_0, \mathbf{C}_f) dt d\mathbf{x}_0 d\epsilon d\mathbf{C}_f. \quad (19)$$

The training objective with noise resembles L_2 regularization. We define two terms:

$$\langle \epsilon|t, \mathbf{x}_0, \mathbf{C}_f \rangle = \int \epsilon p(\epsilon|t, \mathbf{x}_0, \mathbf{C}_f) d\epsilon, \quad \langle \epsilon^2|t, \mathbf{x}_0, \mathbf{C}_f \rangle = \int \epsilon^2 p(\epsilon|t, \mathbf{x}_0, \mathbf{C}_f) d\epsilon. \quad (20)$$

Then, Equation (14) is expanded as follows:

$$\mathcal{L} = \int \int \int \int \int \{y(\mathbf{C}_f) - \langle \epsilon|t, \mathbf{x}_0, \mathbf{C}_f \rangle\}^2 p(\epsilon|t, \mathbf{x}_0, \mathbf{C}_f) p(t, \mathbf{x}_0, \mathbf{C}_f) dt d\mathbf{x}_0 d\epsilon d\mathbf{C}_f + \int \int \int \int \int \{ \langle \epsilon^2|t, \mathbf{x}_0, \mathbf{C}_f \rangle - \langle \epsilon|t, \mathbf{x}_0, \mathbf{C}_f \rangle^2 \} p(\epsilon|t, \mathbf{x}_0, \mathbf{C}_f) p(t, \mathbf{x}_0, \mathbf{C}_f) dt d\mathbf{x}_0 d\epsilon d\mathbf{C}_f. \quad (21)$$

Observe that in Equation (21), only the first integral term involves the parameters of a neural network (i.e., $y(\mathbf{C}_f) = \epsilon_\theta(\mathbf{x}_t, t, \mathbf{C}_f)$, which is the denoising network to be trained), while the second term only depends on the ground truth noise. Therefore, \mathcal{L} is minimized when $y(\mathbf{C}_f) = \langle \epsilon|t, \mathbf{x}_0, \mathbf{C}_f \rangle$.

Also, recall that $\tilde{\mathcal{L}} = \mathcal{L} + \eta^2 \mathcal{L}^R$ by Equation (18). Consider the second term of \mathcal{L}^R in Equation (19) and denote it as \mathcal{L}_2^R . Then, \mathcal{L}_2^R can be rewritten as follows:

$$\mathcal{L}_2^R = \int \int \int \int \sum_i \{y(\mathbf{C}_f) - \langle \epsilon|t, \mathbf{x}_0, \mathbf{C}_f \rangle\} \frac{\partial^2 y}{\partial \mathbf{C}_{f,i}^2} p(\epsilon|t, \mathbf{x}_0, \mathbf{C}_f) p(t, \mathbf{x}_0, \mathbf{C}_f) dt d\mathbf{x}_0 d\epsilon d\mathbf{C}_f \quad (22)$$

Therefore, when \mathcal{L} is minimized at $y(\mathbf{C}_f) = \langle \epsilon|t, \mathbf{x}_0, \mathbf{C}_f \rangle$, $\mathcal{L}_2^R = 0$. As a result, in this case, \mathcal{L}^R can be rewritten to:

$$\mathcal{L}^R = \int \int \int \sum_i \left(\frac{\partial y}{\partial \mathbf{C}_{f,i}} \right)^2 p(t, \mathbf{x}_0, \mathbf{C}_f) dt d\mathbf{x}_0 d\mathbf{C}_f, \quad (23)$$

which is in the Tikhonov form. \square

6 Experiments

6.1 Experimental Settings

Datasets We evaluate the proposed model with seven real-world datasets, as summarized in Table 2. See Appendix A.2 for a detailed description of the datasets. These datasets have been chosen for their large number of feature dimensions relative to the number of rows.

Competitors We compare CtrTab with six models including state-of-the-art (SOTA) diffusion-based tabular data synthesis models: **SMOTE** [Chawla *et al.*, 2002], **TVAE** [Xu *et al.*, 2019], **CTGAN** [Xu *et al.*, 2019], **TabDDPM** [Kotelnikov *et al.*, 2023], **RelDDPM** [Liu *et al.*, 2024], and **TabSyn** [Zhang *et al.*, 2024] (SOTA). More details about these models can be found in Appendix A.2.

Implementation Details All experiments were conducted on a virtual machine with a 12-core Intel(R) Xeon(R) Gold 6326 CPU (2.90 GHz), 32 GB of RAM, and an NVIDIA A100 GPU. We implement CtrTab and all competitor models using Python. For the competitors, we adopt the same hyperparameter settings as specified in the TabSyn paper [Zhang

Method	GE	CL	MA	ED	UN	Avg. Gap	UG	EG	Avg. Gap
	AUC \uparrow	% \downarrow	RMSE \downarrow	RMSE \downarrow	% \downarrow				
Real	0.896	1	0.999	0.990	0.986	0%	0.036	0.115	0%
SMOTE	<u>0.865</u>	0.999	<u>0.996</u>	0.990	0.976	0.98%	<u>0.132</u>	<u>0.118</u>	134.638%
TVAE	-	-	-	0.825	0.819	16.80%	0.775	0.219	1071.606%
CTGAN	0.133	0.653	0.765	0.383	0.534	50.09%	0.754	0.266	1062.874%
TabDDPM	0.504	0.550	0.805	0.459	0.618	39.83%	2.216	0.346	3128.212%
RelDDPM	0.839	0.665	0.687	0.981	<u>0.930</u>	15.54%	0.463	0.122	596.099%
TabSyn	0.791	<u>0.984</u>	<u>0.996</u>	0.952	0.864	5.97%	0.267	0.166	343.007%
CtrTab (Ours)	0.873	0.999	0.999	<u>0.989</u>	0.976	0.76%	0.069	0.115	45.83%
	F1 \uparrow	% \downarrow	R2 \uparrow	R2 \uparrow	% \downarrow				
Real	0.637	0.991	0.993	0.928	0.923	0%	0.998	0.646	0%
SMOTE	<u>0.598</u>	<u>0.968</u>	<u>0.991</u>	<u>0.919</u>	<u>0.889</u>	2.66%	<u>0.970</u>	<u>0.628</u>	<u>2.80%</u>
TVAE	-	-	-	0.673	0.604	31.02%	< 0	< 0	-
CTGAN	0.465	0.190	0.884	0.404	0.580	42.49%	0.031	< 0	96.89%
TabDDPM	0.092	0.018	0.872	0.546	0.620	53.98%	< 0	< 0	-
RelDDPM	0.554	0.334	0.871	0.905	0.841	20.60%	0.634	0.603	21.56%
TabSyn	0.450	0.845	0.983	0.849	0.711	15.32%	0.879	0.270	35.06%
CtrTab (Ours)	0.614	0.985	0.994	0.922	0.902	1.45%	0.992	0.648	0.46%

Table 1: Machine learning test results: The GE, CL, MA, ED, and UN datasets are used for classification, with results in AUC and F1. The UG and EG datasets are for regression, with results in RMSE and R2. Symbol ‘-’ indicates cases where the generative model collapsed, resulting in only a single class of generated samples, or negative R2 values such that the average gap becomes invalid. The best results are in boldface, while the second best are underlined.

Dataset	#Train	#Test	#Num	#Cat	#Total	Task	$N/2^D$
Gesture (GE)	7,898	1,975	32	0	32	Multi	$9.19e^{-7}$
Clean2 (CL)	5,278	1,320	166	2	168	Binary	$7.05e^{-48}$
Malware (MA)	3,572	892	241	0	241	Binary	$5.05e^{-70}$
Education (ED)	2,635	659	52	2	54	Binary	$7.31e^{-14}$
Unemployment (UN)	2,621	656	97	2	99	Binary	$2.07e^{-27}$
Unemploymentreg (UG)	2,621	656	97	2	99	Regres	$2.07e^{-27}$
Educationreg (EG)	2,635	659	52	2	54	Regres	$7.31e^{-14}$

Table 2: Datasets: #Train and #Test refer to the numbers of training and testing rows. #Num and #Cat refer to the numbers of numerical and categorical features, while #Total refers to their sum; ‘Task’ specifies the target downstream tasks, where ‘Multi’ means multi-class classification, ‘Binary’ means binary classification, and ‘Regres’ means regression; $N/2^D$ represents the data sparsity, where $N = \#Train$ and D is the data dimensionality.

et al., 2024]. CtrTab uses the SOTA model TabSyn (score-based SDE-based) as its denoising network by default, while we have also tested an implementation of RelDDPM (DDPM-based). We train it with the AdamW optimizer [Loshchilov and Hutter, 2019] using a learning rate of 0.005 and weight decay of 0.00001 with 30,000 training steps. The noise scales on the seven datasets are 0.03, 0.05, 0.05, 0.005, 0.005, 0.005, and 0.01, respectively, which are tuned in the range of [0.005, 0.05] for high model effectiveness.

6.2 Results

Machine Learning Tests Following existing studies [Kim *et al.*, 2023; Lee *et al.*, 2023; Zhang *et al.*, 2024], we test the effectiveness of CtrTab mainly through machine learning tasks: (1) We train each model with the training set of each dataset. (2) Once trained, we use each model to syn-

thesize a dataset of the same size of the respective training set. (3) We use the original training set and the synthesized set to separately train a downstream classification or regression model (XGBoost and XGBoostRegressor, ‘**downstream model**’ for short hereafter). (4) We evaluate the performance of these trained downstream models on the test set.

For the classification datasets, we report the Area Under the Curve (AUC) and F1 score (F1). For the regression datasets, we report the Root Mean Squared Error (RMSE) and the R-Squared measure (R2).

Table 1 summarizes the results, where ‘Real’ denotes the performance of the downstream model trained on the original data; each model (e.g., our CtrTab) denotes the performance of the downstream model trained on the data synthesized by that model. ‘Avg. Gap’ denotes the average (relative) performance gap between a model and ‘Real’, average across the same type (classification or regression) of datasets. A smaller average gap means a better model, i.e., the model synthesizes data that better fits the original data distribution.

Our model CtrTab reports the best results in almost all cases, except on ED, where SMOTE is marginally higher in AUC. The average gap in AUC, F1, RMSE, and R2 of CtrTab are 22.45%, 45.49%, 65.96%, and 83.57% lower than those of the best baseline model (SMOTE), respectively. Comparing with the SOTA model TabSyn, the performance gains are even higher, i.e., 87.27%, 90.54%, 86.64%, and 98.69%.

These results demonstrate the challenges for the existing diffusion-based models to learn from sparse, high-dimensional tabular data, and the effectiveness of CtrTab in addressing such challenges. SMOTE, while being an early model, shows high effectiveness, because it generates new

samples through adding noise (directly) to existing samples which resembles our idea. TVAE and CTGAN are based on VAE and GAN, which also suffer from the data sparsity issue.

Following the TabSyn paper, to ensure that CtrTab does not simply replicate the training data, we further measure the Distance to Closest Records (DCR) scores of CtrTab and the best baseline SMOTE, which denote the probability that a synthesized sample finds its closest (by L_1 distance) sample in the training set (rather than the testing set). For an ideal model, its DCR scores should be close to 0.5 (i.e., the synthesized samples have good chances to be similar to both the training and the test sets). We report the normalized DCR scores (NDCR, smaller the better) calculated as $|DCR - 0.5|$ in Table 3. CtrTab outperforms SMOTE in six out of the seven datasets, achieving NDCR values that are 1.69% (0.466 vs. 0.474) smaller on average. The NDCR values suggest that CtrTab does not replicate the training data, which is an important property for data release application scenarios.

For the other baselines, their DCR values are lower since their synthesized data do not fit the original data distribution as shown above. We omit those values for conciseness.

Method	GE	CL	MA	ED	UN	UG	EG	Average
SMOTE	0.477	0.500	0.342	0.500	0.500	0.500	0.500	0.474
CtrTab	0.497	0.473	0.319	0.492	0.499	0.490	0.490	0.466

Table 3: DCR results (smaller values are preferred).

Ablation Study CtrTab adds a control module to TabSyn. We further show the importance of the control module by comparing CtrTab with three alternative variants of TabSyn: (1) **Train** $\times 2$ doubles the number of training epochs for TabSyn. (2) **Data** $\times 2$ duplicates each training sample with a Laplace noise of scale 0.01. (3) **Model** $\times 2$ duplicates each training sample as above and doubles the number of model parameters by expanding the hidden layers of TabSyn to match that of CtrTab (CtrTab is $1.8\times$ the size of TabSyn).

We repeat the machine learning tests as above and report the results in F1 and R2 in Table 4. Results in AUC and RMSE share similar patterns and can be found in Appendix A.3. CtrTab outperforms all these variants consistently, confirming the importance of the control module and is consistent with our theoretical analysis.

Method	GE	CL	MA	ED	UN	UG	EG	Average
Metric	F1 \uparrow	R2 \uparrow	R2 \uparrow	-				
Train $\times 2$	0.443	0.831	0.988	0.852	0.698	0.860	0.390	0.746
Data $\times 2$	0.463	0.871	0.987	0.865	0.820	0.937	0.458	0.801
Model $\times 2$	0.522	0.872	0.988	0.892	0.816	0.884	0.569	0.822
CtrTab	0.614	0.985	0.994	0.922	0.902	0.992	0.648	0.858

Table 4: Ablation study results, comparing with variants of TabSyn.

Impact of Noise Type. We also replace Laplace noise in our control module with Gaussian and uniform noise. We find that while using Laplace noise typically leads to the best downstream model accuracy, the gain is often not too large.

This confirms the robustness of CtrTab and the effectiveness of using Laplace noise. Detailed results are in Appendix A.3.

Parameter Study Figure 4a shows the downstream model accuracy (F1 and R2) when the Laplace noise scale in CtrTab is varied from 0.001 to 1000. As the noise scale increases, the model accuracy gradually decreases at start due to the impact of regularization controlled by the noise scale (variance), which follows the theoretical results shown in Section 5. When the noise becomes too large, the control module of the model gradually fails, the regularization becomes ineffective, and the model’s performance converges to that of the original diffusion model. As a result, the curve starts to rise.

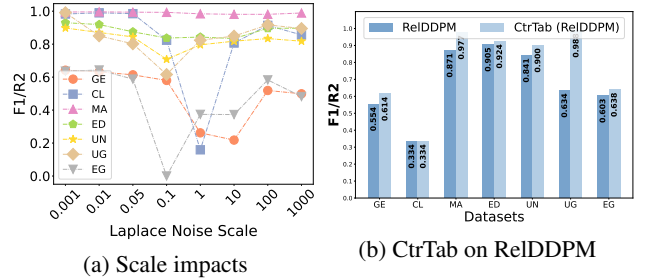


Figure 4: Scale and Applicability Results.

Control Module Applicability Our control module is not limited to be used with TabSyn. In our final set of experiments, we integrate the control module with another model, ReIDDPM, which is a representative DDPM-based model. The downstream model accuracy (F1 and R2) results are shown in Figure 4b, where CtrTab+ReIDDPM also outperforms ReIDDPM consistently. This verifies the applicability of our control module to different diffusion models.

Additional Results In the appendix, we have included the AUC and RMSE results of CtrTab and three variants of TabSyn on seven datasets, the generation performance on the denser datasets with different sample proportions between SMOTE, TabSyn, and CtrTab, a comparison of machine learning test results on non-high-dimensional datasets between TabSyn and CtrTab, the distribution visualization results of the baselines and CtrTab, the impact of intrinsic dimensionality on distribution differences, and the impact of different noise levels to CtrTab on generation performance.

7 Conclusion

We proposed CtrTab, a model designed to enhance the fitting capability of diffusion generative models on high-dimensional tabular data with limited samples. Through an explicit noise-conditioning control and training with a method similar to L_2 regularization, CtrTab synthesizes high-quality tabular data as evidenced by experiments over seven real datasets. The results show that machine learning models trained with data synthesized by CtrTab is much more accurate than those trained with data synthesized by existing models including the SOTA model, with a performance gain of over 80% on average.

Ethical Statement

We present a model for tabular data synthesis. While the proposed model could learn biased information from training data, there are no specific ethical concerns towards the model beyond those common to machine learning models.

References

- [Aggarwal and Yu, 2004] Charu C. Aggarwal and Philip S. Yu. A condensation approach to privacy preserving data mining. In *EDBT*, pages 183–199, 2004.
- [AGRICULTURE, 2023] U.S. DEPARTMENT OF AGRICULTURE. Economic Research Service, 2023. <https://www.ers.usda.gov/data-products/county-level-data-sets/county-level-data-sets-download-data/>.
- [Arjovsky *et al.*, 2017] Martin Arjovsky, Soumith Chintala, and Léon Bottou. Wasserstein generative adversarial networks. In *ICML*, pages 214–223, 2017.
- [Bao *et al.*, 2022] Fan Bao, Chongxuan Li, Jiacheng Sun, and Jun Zhu. Why are conditional generative models better than unconditional ones? In *NeurIPS 2022 Workshop on Score-Based Methods*, 2022.
- [Barak *et al.*, 2007] Boaz Barak, Kamalika Chaudhuri, Cynthia Dwork, Satyen Kale, Frank McSherry, and Kunal Talwar. Privacy, accuracy, and consistency too. In *PODS*, pages 273–282, 2007.
- [Bishop, 1995] Chris M. Bishop. Training with noise is equivalent to Tikhonov regularization. *Neural Computation*, 7(1):108–116, 1995.
- [Bishop, 2006] Christopher M. Bishop. *Pattern Recognition and Machine Learning (Information Science and Statistics)*. Springer-Verlag, Berlin, Heidelberg, 2006.
- [Borah and Bhattacharyya, 2020] Parthajit Borah and Dhruva K. Bhattacharyya. TUANDROMD (Tezpur University Android Malware Dataset). UCI Machine Learning Repository, 2020. <https://doi.org/10.24432/C5560H>.
- [Chapman and Jain, 1994] David Chapman and Ajay Jain. Musk (Version 2). UCI Machine Learning Repository, 1994. <https://doi.org/10.24432/C51608>.
- [Chawla *et al.*, 2002] Nitesh V. Chawla, Kevin W. Bowyer, Lawrence O. Hall, and W. Philip Kegelmeyer. SMOTE: Synthetic minority over-sampling technique. *Journal of Artificial Intelligence Research*, 16:321–357, 2002.
- [Chen *et al.*, 2019] Haipeng Chen, Sushil Jajodia, Jing Liu, Noseong Park, Vadim Sokolov, and V. S. Subrahmanian. FakeTables: Using GANs to generate functional dependency preserving tables with bounded real data. In *IJCAI*, pages 2074–2080, 2019.
- [Dwork and Roth, 2014] Cynthia Dwork and Aaron Roth. The algorithmic foundations of differential privacy. *Foundations and Trends in Theoretical Computer Science*, 9, 2014.
- [Fang *et al.*, 2024] Liancheng Fang, Aiwei Liu, Hengrui Zhang, Henry Peng Zou, Weizhi Zhang, and Philip S. Yu. RES-RAG: Residual-aware RAG for realistic tabular data generation. In *NeurIPS 2024 Third Table Representation Learning Workshop*, 2024.
- [Ho and Salimans, 2021] Jonathan Ho and Tim Salimans. Classifier-free diffusion guidance. In *NeurIPS 2021 Workshop on Deep Generative Models and Downstream Applications*, 2021.
- [Ho *et al.*, 2020] Jonathan Ho, Ajay Jain, and Pieter Abbeel. Denoising diffusion probabilistic models. In H. Larochelle, M. Ranzato, R. Hadsell, M.F. Balcan, and H. Lin, editors, *Advances in Neural Information Processing Systems*, volume 33, pages 6840–6851. Curran Associates, Inc., 2020.
- [Kim *et al.*, 2021] Jayoung Kim, Jinsung Jeon, Jaehoon Lee, Jihyeon Hyeong, and Noseong Park. OCT-GAN: Neural ODE-based conditional tabular GANs. In *WWW*, pages 1506–1515, 2021.
- [Kim *et al.*, 2023] Jayoung Kim, Chaejeong Lee, and Noseong Park. STasy: Score-based tabular data synthesis. In *ICLR*, 2023.
- [Kotelnikov *et al.*, 2023] Akim Kotelnikov, Dmitry Baranchuk, Ivan Rubachev, and Artem Babenko. TabDDPM: Modelling tabular data with diffusion models. In *ICML*, pages 17564–17579, 2023.
- [Lee *et al.*, 2023] Chaejeong Lee, Jayoung Kim, and Noseong Park. CoDi: Co-evolving contrastive diffusion models for mixed-type tabular synthesis. In *ICML*, pages 18940–18956, 2023.
- [Li *et al.*, 2014] Haoran Li, Li Xiong, Lifan Zhang, and Xiaojian Jiang. DPSynthesizer: Differentially private data synthesizer for privacy preserving data sharing. *Proceedings of the VLDB Endowment*, 7(13):1677–1680, 2014.
- [Liu *et al.*, 2024] Tongyu Liu, Ju Fan, Nan Tang, Guoliang Li, and Xiaoyong Du. Controllable tabular data synthesis using diffusion models. *Proceedings of the ACM on Management of Data*, 2(1), 2024.
- [Loshchilov and Hutter, 2019] Ilya Loshchilov and Frank Hutter. Decoupled weight decay regularization. In *ICLR*, 2019.
- [Madeo *et al.*, 2013] Renata C. B. Madeo, Clodoaldo A. M. Lima, and Sarajane M. Peres. Gesture unit segmentation using support vector machines: Segmenting gestures from rest positions. In *ACM Symposium on Applied Computing*, pages 46–52, 2013.
- [Ng, 2004] Andrew Y. Ng. Feature selection, l_1 vs. l_2 regularization, and rotational invariance. In *ICML, ICML '04*, page 78, 2004.
- [Park *et al.*, 2013] Yubin Park, Joydeep Ghosh, and Mallikarjun Shankar. Perturbed Gibbs samplers for generating large-scale privacy-safe synthetic health data. In *IEEE International Conference on Healthcare Informatics*, pages 493–498, 2013.
- [Park *et al.*, 2018] Noseong Park, Mahmoud Mohammadi, Kshitij Gorde, Sushil Jajodia, Hongkyu Park, and Youngmin Kim. Data synthesis based on generative adver-

- sarial networks. *Proceedings of the VLDB Endowment*, (10):1071–1083, 2018.
- [Shi *et al.*, 2024] Juntong Shi, Harper Hua, Minkai Xu, Hengrui Zhang, Stefano Ermon, and Jure Leskovec. TabDiff: A unified diffusion model for multi-modal tabular data generation. In *NeurIPS 2024 Table Representation Learning Workshop*, 2024.
- [Shorten and Khoshgoftaar, 2019] Connor Shorten and Taghi M. Khoshgoftaar. A survey on image data augmentation for deep learning. *Journal of Big Data*, 6, 2019.
- [Song *et al.*, 2021] Yang Song, Jascha Sohl-Dickstein, Diederik P Kingma, Abhishek Kumar, Stefano Ermon, and Ben Poole. Score-based generative modeling through stochastic differential equations. In *ICLR*, 2021.
- [Valiant, 1984] L. G. Valiant. A theory of the learnable. *Communications of the ACM*, 27(11):1134–1142, 1984.
- [Wang *et al.*, 2024] Yuxin Wang, Duanyu Feng, Yongfu Dai, Zhengyu Chen, Jimin Huang, Sophia Ananiadou, Qianqian Xie, and Hao Wang. HARMONIC: Harnessing LLMs for tabular data synthesis and privacy protection. In *NeurIPS 2024 Datasets and Benchmarks Track*, 2024.
- [Webb, 1994] A.R. Webb. Functional approximation by feed-forward networks: A least-squares approach to generalization. *IEEE Transactions on Neural Networks*, 5(3):363–371, 1994.
- [Wen *et al.*, 2022] Bingyang Wen, Yupeng Cao, Fan Yang, Koduvayur Subbalakshmi, and Rajarathnam Chandramouli. Causal-TGAN: Modeling tabular data using causally-aware GAN. In *ICLR Workshop on Deep Generative Models for Highly Structured Data*, 2022.
- [Xu *et al.*, 2019] Lei Xu, Maria Skoularidou, Alfredo Cuesta-Infante, and Kalyan Veeramachaneni. Modeling tabular data using conditional GAN. In *NeurIPS*, pages 7335–7345, 2019.
- [Zhang *et al.*, 2014] Jun Zhang, Graham Cormode, Cecilia M. Procopiuc, Divesh Srivastava, and Xiaokui Xiao. PrivBayes: Private data release via Bayesian networks. In *SIGMOD*, pages 1423–1434, 2014.
- [Zhang *et al.*, 2023] Lvmin Zhang, Anyi Rao, and Maneesh Agrawala. Adding conditional control to text-to-image diffusion models. In *ICCV*, pages 3836–3847, 2023.
- [Zhang *et al.*, 2024] Hengrui Zhang, Jiani Zhang, Balasubramaniam Srinivasan, Zhengyuan Shen, Xiao Qin, Christos Faloutsos, Huzefa Rangwala, and George Karypis. Mixed-type tabular data synthesis with score-based diffusion in latent space. In *ICLR*, 2024.
- [Zhao *et al.*, 2023] Zilong Zhao, Aditya Kunar, Robert Birke, Hiek Van der Scheer, and Lydia Y Chen. CTABGAN+: Enhancing tabular data synthesis. *Frontiers in Big Data*, 6, 2023.

A Appendix

A.1 Detailed Proofs

In this section, we give a detailed formal proof for Theorem 1 in Section 5. For easy reference, we restate the theorem here:

Theorem 1. *Let the training objective of CtrTab be minimizing $\mathcal{L} = \mathbb{E}_{\mathbf{x}_0, t, \epsilon, \mathbf{C}_f} \|\epsilon - \epsilon_\theta(\mathbf{x}_t, t, \mathbf{C}_f)\|^2$, and let the training objective with a noise added condition be minimizing $\tilde{\mathcal{L}} = \mathbb{E}_{\mathbf{x}_0, t, \epsilon, \mathbf{C}_f, \tilde{\epsilon}} \|\epsilon - \epsilon_\theta(\mathbf{x}_t, t, \mathbf{C}_f + \tilde{\epsilon})\|^2$, where $\tilde{\epsilon}$ is a noise drawn from a distribution with mean 0 and variance η^2 . Then, $\tilde{\mathcal{L}} = \mathcal{L} + \eta^2 \mathcal{L}^R$ holds, where \mathcal{L}^R is a regularization term in the Tikhonov form.*

Proof. **Expansion of the training objectives.**

For simplicity, define $y(\mathbf{C}_f) = \epsilon_\theta(x_t, t, \mathbf{C}_f)$. Then $\mathcal{L} = \mathbb{E}_{x_0, t, \epsilon, \mathbf{C}_f} \|\epsilon - \epsilon_\theta(x_t, t, \mathbf{C}_f)\|^2$ can be expanded as follows:

$$\begin{aligned} \mathcal{L} &= \int \int \int \int \{y(\mathbf{C}_f) - \epsilon\}^2 p(t, x_0, \epsilon, \mathbf{C}_f) dt dx_0 d\epsilon d\mathbf{C}_f \\ &= \int \int \int \int \{y(\mathbf{C}_f) - \epsilon\}^2 p(\epsilon|t, x_0, \mathbf{C}_f) p(t, x_0, \mathbf{C}_f) dt dx_0 d\epsilon d\mathbf{C}_f \end{aligned} \quad (24)$$

Next, we expand $\tilde{\mathcal{L}} = \mathbb{E}_{x_0, t, \epsilon, \mathbf{C}_f, \tilde{\epsilon}} \|\epsilon - \epsilon_\theta(x_t, t, \mathbf{C}_f + \tilde{\epsilon})\|^2$ as:

$$\begin{aligned} \tilde{\mathcal{L}} &= \int \int \int \int \int \{y(\mathbf{C}_f + \tilde{\epsilon}) - \epsilon\}^2 p(t, x_0, \epsilon, \mathbf{C}_f, \tilde{\epsilon}) dt dx_0 d\epsilon d\mathbf{C}_f d\tilde{\epsilon} \\ &= \int \int \int \int \int \{y(\mathbf{C}_f + \tilde{\epsilon}) - \epsilon\}^2 p(t, x_0, \epsilon, \mathbf{C}_f) p(\tilde{\epsilon}) dt dx_0 d\epsilon d\mathbf{C}_f d\tilde{\epsilon} \\ &\quad (\tilde{\epsilon} \text{ is independent to other variables}) \\ &= \int \int \int \int \int \{y(\mathbf{C}_f + \tilde{\epsilon}) - \epsilon\}^2 p(\epsilon|t, x_0, \mathbf{C}_f) p(t, x_0, \mathbf{C}_f) p(\tilde{\epsilon}) dt dx_0 d\epsilon d\mathbf{C}_f d\tilde{\epsilon} \\ &\quad (\text{Decomposition of joint distribution}) \end{aligned} \quad (25)$$

Some Preliminaries. Expanding $y(\mathbf{C}_f + \tilde{\epsilon})$ with Taylor series, and assuming the noise amplitude is small such that any term of order $O(\tilde{\epsilon}^3)$ or higher can be neglected, then we have:

$$y(\mathbf{C}_f + \tilde{\epsilon}) = y(\mathbf{C}_f) + \sum_i \tilde{\epsilon}_i \left. \frac{\partial y}{\partial C_{f,i}} \right|_{\tilde{\epsilon}=0} + \frac{1}{2} \sum_i \sum_j \tilde{\epsilon}_i \tilde{\epsilon}_j \left. \frac{\partial^2 y}{\partial C_{f,i} \partial C_{f,j}} \right|_{\tilde{\epsilon}=0} + O(\tilde{\epsilon}^3) \quad (26)$$

By the fact that $\tilde{\epsilon}$ is chosen from a distribution with mean 0 and variance η^2 , we have the following equalities:

$$\int \tilde{\epsilon}_i p(\tilde{\epsilon}) d\tilde{\epsilon} = 0 \quad \int \tilde{\epsilon}_i \tilde{\epsilon}_j p(\tilde{\epsilon}) d\tilde{\epsilon} = \eta^2 \delta_{ij}, \text{ where } \delta_{ij} = \begin{cases} 1 & i = j \\ 0 & i \neq j \end{cases} \quad (27)$$

Showing that the noised training objective takes the form of regularization. By substituting Equation (26) to Equation (25), we get:

$$\begin{aligned} \tilde{\mathcal{L}} &= \int \int \int \int \int \left\{ y(\mathbf{C}_f) + \sum_i \tilde{\epsilon}_i \left. \frac{\partial y}{\partial C_{f,i}} \right|_{\tilde{\epsilon}=0} + \frac{1}{2} \sum_i \sum_j \tilde{\epsilon}_i \tilde{\epsilon}_j \left. \frac{\partial^2 y}{\partial C_{f,i} \partial C_{f,j}} \right|_{\tilde{\epsilon}=0} + O(\tilde{\epsilon}^3) - \epsilon \right\}^2 p(\epsilon|t, x_0, \mathbf{C}_f) \\ &\quad p(t, x_0, \mathbf{C}_f) p(\tilde{\epsilon}) dt dx_0 d\epsilon d\mathbf{C}_f d\tilde{\epsilon} \text{ (substitution)} \end{aligned} \quad (28)$$

$$\begin{aligned} &= \int \int \int \int \int \left\{ (y(\mathbf{C}_f) - \epsilon) + \sum_i \tilde{\epsilon}_i \left. \frac{\partial y}{\partial C_{f,i}} \right|_{\tilde{\epsilon}=0} + \frac{1}{2} \sum_i \sum_j \tilde{\epsilon}_i \tilde{\epsilon}_j \left. \frac{\partial^2 y}{\partial C_{f,i} \partial C_{f,j}} \right|_{\tilde{\epsilon}=0} \right\}^2 p(\epsilon|t, x_0, \mathbf{C}_f) p(t, x_0, \mathbf{C}_f) \\ &\quad p(\tilde{\epsilon}) dt dx_0 d\epsilon d\mathbf{C}_f d\tilde{\epsilon} \text{ (rearrange the terms inside the squared expression and omitted the } O(\tilde{\epsilon}^3) \text{ term)} \end{aligned} \quad (29)$$

$$\begin{aligned} &= \int \int \int \int \int \left\{ \underbrace{(y(\mathbf{C}_f) - \epsilon)^2}_{(A)} + \underbrace{\left(\sum_i \tilde{\epsilon}_i \left. \frac{\partial y}{\partial C_{f,i}} \right|_{\tilde{\epsilon}=0} \right)^2}_{(B)} + \underbrace{\left(\frac{1}{2} \sum_i \sum_j \tilde{\epsilon}_i \tilde{\epsilon}_j \left. \frac{\partial^2 y}{\partial C_{f,i} \partial C_{f,j}} \right|_{\tilde{\epsilon}=0} \right)^2}_{(C)} + \right. \\ &\quad \left. \underbrace{2(y(\mathbf{C}_f) - \epsilon) \sum_i \tilde{\epsilon}_i \left. \frac{\partial y}{\partial C_{f,i}} \right|_{\tilde{\epsilon}=0}}_{(D)} + \underbrace{(y(\mathbf{C}_f) - \epsilon) \sum_i \sum_j \tilde{\epsilon}_i \tilde{\epsilon}_j \left. \frac{\partial^2 y}{\partial C_{f,i} \partial C_{f,j}} \right|_{\tilde{\epsilon}=0}}_{(E)} + \underbrace{\sum_i \tilde{\epsilon}_i \left. \frac{\partial y}{\partial C_{f,i}} \right|_{\tilde{\epsilon}=0} \sum_i \sum_j \tilde{\epsilon}_i \tilde{\epsilon}_j \left. \frac{\partial^2 y}{\partial C_{f,i} \partial C_{f,j}} \right|_{\tilde{\epsilon}=0}}_{(F)} \right\} \end{aligned}$$

$$p(\epsilon|t, x_0, C_f)p(t, x_0, C_f)p(\tilde{\epsilon}) dt dx_0 d\epsilon dC_f d\tilde{\epsilon} \text{ (expansion of the square term)} \quad (30)$$

$$= \int \int \int \int \int \underbrace{\{ (y(C_f) - \epsilon)^2 \}}_{(A)} + \underbrace{\left(\sum_i \tilde{\epsilon}_i \frac{\partial y}{\partial C_{f,i}} \Big|_{\tilde{\epsilon}=0} \right)^2}_{(B)} + \underbrace{2(y(C_f) - \epsilon) \sum_i \tilde{\epsilon}_i \frac{\partial y}{\partial C_{f,i}} \Big|_{\tilde{\epsilon}=0}}_{(D)} + \underbrace{(y(C_f) - \epsilon) \sum_i \sum_j \tilde{\epsilon}_i \tilde{\epsilon}_j \frac{\partial^2 y}{\partial C_{f,i} \partial C_{f,j}} \Big|_{\tilde{\epsilon}=0}}_{(E)} \} p(\epsilon|t, x_0, C_f)p(t, x_0, C_f)p(\tilde{\epsilon}) dt dx_0 d\epsilon dC_f d\tilde{\epsilon}$$

(omit (C) and (F) as they are of order higher than $O(\tilde{\epsilon}^3)$) (31)

$$= \int \int \int \int \int \underbrace{(y(C_f) - \epsilon)^2}_{(A)} p(\epsilon|t, x_0, C_f)p(t, x_0, C_f)p(\tilde{\epsilon}) dt dx_0 d\epsilon dC_f d\tilde{\epsilon} + \int \int \int \int \int \underbrace{\left(\sum_i \tilde{\epsilon}_i \frac{\partial y}{\partial C_{f,i}} \Big|_{\tilde{\epsilon}=0} \right)^2}_{(B)} p(\epsilon|t, x_0, C_f)p(t, x_0, C_f)p(\tilde{\epsilon}) dt dx_0 d\epsilon dC_f d\tilde{\epsilon} + \int \int \int \int \int \underbrace{2(y(C_f) - \epsilon) \sum_i \tilde{\epsilon}_i \frac{\partial y}{\partial C_{f,i}} \Big|_{\tilde{\epsilon}=0}}_{(D)} p(\epsilon|t, x_0, C_f)p(t, x_0, C_f)p(\tilde{\epsilon}) dt dx_0 d\epsilon dC_f d\tilde{\epsilon} + \int \int \int \int \int \underbrace{(y(C_f) - \epsilon) \sum_i \sum_j \tilde{\epsilon}_i \tilde{\epsilon}_j \frac{\partial^2 y}{\partial C_{f,i} \partial C_{f,j}} \Big|_{\tilde{\epsilon}=0}}_{(E)} p(\epsilon|t, x_0, C_f)p(t, x_0, C_f)p(\tilde{\epsilon}) dt dx_0 d\epsilon dC_f d\tilde{\epsilon}$$

(distribute the integrals) (32)

$$= \int \int \int \int \underbrace{(y(C_f) - \epsilon)^2}_{(A)} p(\epsilon|t, x_0, C_f)p(t, x_0, C_f) dt dx_0 d\epsilon dC_f \text{ (omit } \int p(\tilde{\epsilon}) d\tilde{\epsilon} \text{ as equals 1)}$$

$$+ \eta^2 \int \int \int \int \sum_i \left(\frac{\partial y}{\partial C_{f,i}} \right)^2 p(\epsilon|t, x_0, C_f)p(t, x_0, C_f) dt dx_0 d\epsilon dC_f$$

(change $\int \tilde{\epsilon}_i^2 p(\tilde{\epsilon}) d\tilde{\epsilon} = \text{Var}(\tilde{\epsilon}_i) = \eta^2$ in (B) from Equality (27))

$$+ \eta^2 \int \int \int \int \sum_i (y(C_f) - \epsilon) \frac{\partial^2 y}{\partial C_{f,i}^2} p(\epsilon|t, x_0, C_f)p(t, x_0, C_f) dt dx_0 d\epsilon dC_f$$

(omit (D) term as it contains $\int \tilde{\epsilon}_i P(\tilde{\epsilon}) d\tilde{\epsilon}$, which is the expectation of $\tilde{\epsilon}$ equal to 0 by Equality (27), and

$$\text{change (E) as } \int \tilde{\epsilon}_i \tilde{\epsilon}_j P(\tilde{\epsilon}) d\tilde{\epsilon} = \eta^2 \delta_{ij} = \int \tilde{\epsilon}_i^2 P(\tilde{\epsilon}) d\tilde{\epsilon} = \text{Var}(\tilde{\epsilon}_i) = \eta^2) \quad (33)$$

$$= \mathcal{L} + \eta^2 \mathcal{L}^R, \quad (34)$$

where

$$\mathcal{L}^R = \int \int \int \int \sum_i \left\{ \left(\frac{\partial y}{\partial C_{f,i}} \right)^2 + (y(C_f) - \epsilon) \frac{\partial^2 y}{\partial C_{f,i}^2} \right\} p(\epsilon|t, x_0, C_f)p(t, x_0, C_f) dt dx_0 d\epsilon dC_f \quad (35)$$

Showing that the noised training objective takes a form similar to L_2 regularization. We define two terms:

$$\langle \epsilon|t, x_0, c_f \rangle = \int \epsilon p(\epsilon|t, x_0, c_f) d\epsilon \quad \langle \epsilon^2|t, x_0, c_f \rangle = \int \epsilon^2 p(\epsilon|t, x_0, c_f) d\epsilon \quad (36)$$

Then expand Equation (24) as follows:

$$\mathcal{L} = \int \int \int \int \{ (y(C_f) - \epsilon)^2 \} p(\epsilon|t, x_0, C_f)p(t, x_0, C_f) dt dx_0 d\epsilon dC_f$$

$$\begin{aligned}
&= \int \int \int \int \{y(C_f)^2 - 2y(C_f)\epsilon + \epsilon^2\}p(\epsilon|t, x_0, C_f)p(t, x_0, C_f) dt dx_0 d\epsilon dC_f \text{ (expand the square term)} \\
&= \underbrace{\int \int \int \int y(C_f)^2 p(\epsilon|t, x_0, C_f)p(t, x_0, C_f) dt dx_0 d\epsilon dC_f}_{(A)} - 2 \underbrace{\int \int \int \int y(C_f)\epsilon p(\epsilon|t, x_0, C_f)p(t, x_0, C_f) dt dx_0 d\epsilon dC_f}_{(B)} \\
&+ \underbrace{\int \int \int \int \epsilon^2 p(\epsilon|t, x_0, C_f)p(t, x_0, C_f) dt dx_0 d\epsilon dC_f}_{(C)} \text{ (expand terms)} \\
&= \underbrace{\int \int \int y(C_f)^2 p(t, x_0, C_f) dt dx_0 dC_f}_{(A)} - 2 \underbrace{\int \int \int y(C_f)\langle\epsilon|t, x_0, c_f\rangle p(t, x_0, C_f) dt dx_0 dC_f}_{(B)} \\
&+ \underbrace{\int \int \int \langle\epsilon^2|t, x_0, c_f\rangle P(t, x_0, C_f) dt dx_0 dC_f}_{(C)}
\end{aligned}$$

((A): $\int p(\epsilon|t, x_0, C_f)d\epsilon = 1$, (B): substitute Equation (36), (C): substitute Equation (36))

$$\begin{aligned}
&= \underbrace{\int \int \int y(C_f)^2 p(t, x_0, C_f) dt dx_0 dC_f}_{(A)} - 2 \underbrace{\int \int \int y(C_f)\langle\epsilon|t, x_0, c_f\rangle p(t, x_0, C_f) dt dx_0 dC_f}_{(B)} \\
&+ \underbrace{\int \int \int \{Var(\epsilon|t, x_0, c_f) + \langle\epsilon|t, x_0, c_f\rangle^2\} p(t, x_0, C_f) dt dx_0 dC_f}_{(C)}
\end{aligned}$$

(rewrite (C) with the formula $Var(\epsilon|t, x_0, c_f) = \langle\epsilon^2|t, x_0, c_f\rangle - (\langle\epsilon|t, x_0, c_f\rangle)^2$)

$$= \int \int \int \{y(C_f) - \langle\epsilon|t, x_0, c_f\rangle\}^2 p(t, x_0, C_f) dt dx_0 dC_f + \int \int \int Var(\epsilon|t, x_0, c_f)p(t, x_0, C_f) dt dx_0 dC_f$$

(rearranging and combining terms)

$$\begin{aligned}
&= \int \int \int \int \{y(C_f) - \langle\epsilon|t, x_0, c_f\rangle\}^2 p(\epsilon|t, x_0, C_f)p(t, x_0, C_f) dt dx_0 d\epsilon dC_f + \int \int \int \int \{\langle\epsilon^2|t, x_0, c_f\rangle - \\
&\langle\epsilon|t, x_0, c_f\rangle^2\} p(\epsilon|t, x_0, C_f)p(t, x_0, C_f) dt dx_0 d\epsilon dC_f \text{ (add } \int p(\epsilon|t, x_0, C_f)d\epsilon = 1 \text{ back)} \tag{37}
\end{aligned}$$

Observe that in Equation (37), only the first term involves the parameters of the neural network (recalling that $y(\mathbf{C}_f) = \epsilon_\theta(x_t, t, \mathbf{C}_f)$), while the second term only depends on the ground truth noise. Therefore, according to Equation (37), E is minimized when $y(\mathbf{C}_f) = \langle\epsilon|t, x_0, c_f\rangle$.

Moreover, recall that $\tilde{\mathcal{L}} = \mathcal{L} + \eta^2 \mathcal{L}^R$ by Equation (18). Consider the second term of \mathcal{L}^R in Equation (19) and denote it as \mathcal{L}_2^R . Then \mathcal{L}_2^R can be rewritten as follows:

$$\begin{aligned}
\mathcal{L}_2^R &= \int \int \int \int \sum_i (y(C_f) - \epsilon) \frac{\partial^2 y}{\partial C_{f,i}^2} p(\epsilon|t, x_0, C_f)p(t, x_0, C_f) dt dx_0 d\epsilon dC_f \\
&= \int \int \int \int \sum_i y(C_f) \frac{\partial^2 y}{\partial C_{f,i}^2} p(\epsilon|t, x_0, C_f)p(t, x_0, C_f) dt dx_0 d\epsilon dC_f - \int \int \int \int \sum_i \epsilon \frac{\partial^2 y}{\partial C_{f,i}^2} p(\epsilon|t, x_0, C_f) \\
&p(t, x_0, C_f) dt dx_0 d\epsilon dC_f \text{ (expand)} \\
&= \int \int \int \int \sum_i y(C_f) \frac{\partial^2 y}{\partial C_{f,i}^2} p(\epsilon|t, x_0, C_f)p(t, x_0, C_f) dt dx_0 d\epsilon dC_f - \int \int \int \int \sum_i \langle\epsilon|t, x_0, c_f\rangle \frac{\partial^2 y}{\partial C_{f,i}^2} p(t, x_0, C_f) \\
&dt dx_0 dC_f \text{ (substitute Equation (36))} \\
&= \int \int \int \int \sum_i y(C_f) \frac{\partial^2 y}{\partial C_{f,i}^2} p(\epsilon|t, x_0, C_f)p(t, x_0, C_f) dt dx_0 d\epsilon dC_f - \int \int \int \int \sum_i \langle\epsilon|t, x_0, c_f\rangle \frac{\partial^2 y}{\partial C_{f,i}^2}
\end{aligned}$$

$$\begin{aligned}
& p(\epsilon|t, x_0, C_f)p(t, x_0, C_f) dt dx_0 d\epsilon dC_f \text{ (add back } \int p(\epsilon|t, x_0, C_f)d\epsilon = 1) \\
& = \int \int \int \int \sum_i \{y(C_f) - \langle \epsilon|t, x_0, c_f \rangle\} \frac{\partial^2 y}{\partial C_{f,i}^2} p(\epsilon|t, x_0, C_f)p(t, x_0, C_f) dt dx_0 d\epsilon dC_f \text{ (combine terms)}
\end{aligned} \tag{38}$$

Therefore, when \mathcal{L} is minimized at $y(\mathbf{C}_f) = \langle \epsilon|t, x_0, c_f \rangle$, $\mathcal{L}_2^R = 0$. As a result, in this case, \mathcal{L}^R can be rewritten to:

$$\begin{aligned}
\mathcal{L}^R & = \int \int \int \int \sum_i \left(\frac{\partial y}{\partial C_{f,i}}\right)^2 p(\epsilon|t, x_0, C_f)p(t, x_0, C_f) dt dx_0 d\epsilon dC_f \\
& = \int \int \int \sum_i \left(\frac{\partial y}{\partial C_{f,i}}\right)^2 p(t, x_0, C_f) dt dx_0 dC_f,
\end{aligned} \tag{39}$$

which is in the Tikhonov form. Hence, completing the proof. \square

A.2 Additional Details on Experimental Settings

Datasets We test our model on the following seven datasets:

- **Gesture (GE)** [Madeo *et al.*, 2013] is a dataset from the field of human-computer interaction used for gesture analysis, i.e., gesture phase segmentation which is a multi-class classification task. Each row of the dataset represents the gesture information captured by the device. We use the last categorical column as the class labels while the rest of the columns as the data features for the multi-classification task.
- **Clean2 (CL)** [Chapman and Jain, 1994] is a binary classification dataset from the UCI Machine Learning Repository, used to predict whether new molecules are musk or non-musk. Each row of the dataset represents the exact shape, or conformation, of the molecule. We use the last categorical column as the class labels while the rest of the columns as the data features for the classification task.
- **Malware (MA)** [Borah and Bhattacharyya, 2020] is another binary classification dataset from the UCI Machine Learning Repository, used to predict whether a software is malware or not. Each row of the dataset represents software permission information. We use the last column as the class labels while the rest of the columns as the data features for the classification task.
- **Education (ED)** [AGRICULTURE, 2023] is a dataset from the US Department of Agriculture that provides statistics on the educational attainment of adults aged 25 and older in the USA, across states and counties, from 1970 to 2022. We use this dataset for a binary classification task by transforming the column “Percent of adults with a bachelor’s degree or higher, 2018-22” based on the median value: values greater than the median are marked as label 1, while others are marked as label 0.
- **Unemployment (UN)** [AGRICULTURE, 2023] is a dataset from the US Department of Agriculture that contains median household income for the the states and counties in the USA from 2000 to 2022. We use this dataset for a binary classification task by converting column “County household median income as a percent of State total median household income, 2021” into binary labels, where 1 means “YES” and 0 otherwise.
- **Unemploymentreg (UG)** [AGRICULTURE, 2023] is the same unemployment dataset as above. Now we use the raw values of the column “County household median income as a percent of State total median household income, 2021” to form a regression task.
- **Educationreg (EG)** [AGRICULTURE, 2023] is the same Education dataset as above. Now we use the raw values from the column “Percent of adults with a bachelor’s degree or higher, 2018-22” to form a regression task.

Competitors We compare CtrTab with six models including state-of-the-art (SOTA) diffusion-based tabular data synthesis models:

- **SMOTE** [Chawla *et al.*, 2002] is a traditional yet highly effective oversampling technique proposed to address the class imbalance issue by generating synthetic samples for a minority class. It creates new data samples by interpolating between existing samples of the target minority class to increase their representation in the dataset.
- **TVAE** [Xu *et al.*, 2019] is a variational autoencoder based models for synthesizing tabular data.
- **CTGAN** [Xu *et al.*, 2019] is classical a GAN-based model which uses conditional information and different normalizations to generate data samples while addressing class imbalance and complicated distribution challenges.
- **TabDDPM** [Kotelnikov *et al.*, 2023] is one of the first models that extend diffusion models to tabular data synthesis. It proposes different diffusion processes for different types (i.e., numerical and categorical) of data from a table.
- **RelDDPM** [Liu *et al.*, 2024] is a recent diffusion-based model based on classifier-guidance. It trains an additional classifier to provide supervision signal to guide the data synthesis process towards a given conditional direction.

- **TabSyn** [Zhang *et al.*, 2024] is the SOTA model for tabular data synthesis. It uses a B-VAE to learn an embedding for each sample in a data table, and then it employs a score-based diffusion model for tabular data synthesis using the learned embeddings.

A.3 Additional Experimental Results

Additional Ablation Study As discussed in Section 6.2, we show the results of AUC and RMSE of CtrTab with three alternative variants of TabSyn in Table 5. Specifically, these three TabSyn variants are designed to make the comparison with our CtrTab more fair, where Train $\times 2$ uses double training steps for TabSyn, while Data $\times 2$ and Model $\times 2$ are strengthened versions of Train $\times 2$ by further doubling the size of training data by adding noise to training data, and using twice of parameters for TabSyn, respectively. As shown in Table 5, our CtrTab outperforms all the three competitors on all the seven datasets. It clearly shows the effectiveness of our proposed control module in CtrTab.

Method	GE	CL	MA	ED	UN	UG	EG
Metric	AUC \uparrow	RMSE \downarrow	RMSE \downarrow				
Train $\times 2$	0.795	0.979	0.996	0.958	0.818	0.285	0.151
Data $\times 2$	0.804	0.990	0.998	0.963	0.916	0.192	0.143
Model $\times 2$	0.827	0.990	0.997	0.981	0.919	0.256	0.127
CtrTab	0.873	0.999	0.999	0.989	0.976	0.069	0.115

Table 5: Comparison of TabSyn with 2 \times training steps, TabSyn with additional 1 \times noised data, TabSyn with additional 1 \times noised data and 2 \times parameters, and CtrTab.

Additional results on the impact of training set size We show the additional result about the impact of training set size on the ADU dataset in Table 6. The results demonstrate that CtrTab works well across all different sizes of training data and consistently outperforms the two competitors. Interestingly, from these results, one can see that our CtrTab is robust on the training data size. This demonstrates that CtrTab can enable the model to learn useful information even in low-sample scenarios, thereby synthesizing data that closely matches the real data distribution.

Method	10%	30%	50%	100%
SMOTE	94.03%	93.5%	94.8%	97.5%
TabSyn	94.5%	97.6%	98.1%	98.9%
CtrTab	98.7%	98.4%	98.6%	98.9%

Table 6: Impact of Training Set Size on Generative Model Density Performance for the ADU (the sparsest) Dataset

Applicability on Non-High-Dimensional Datasets We demonstrate the applicability of our module on non-high-dimensional datasets. We adopted the datasets used by TabSyn and compared the performance of TabSyn with our model. For CtrTab, we use a default parameter setting with a scale of 0.1 and a weight of 1 to obtain the results in Table 7. As shown,

Methods	ADU	DEF	SHO	MAL	BEI	NEW	Average Gap
	AUC \uparrow	AUC \uparrow	AUC \uparrow	AUC \uparrow	RMSE \downarrow	RMSE \downarrow	% \downarrow
Real	0.927	0.770	0.926	0.946	0.432	0.842	0%
TabSyn	0.911	0.762	0.920	0.934	0.695	0.854	11.16%
CtrTab	0.912	0.769	0.923	0.933	0.609	0.859	7.74%

Table 7: Downstream results on non-high-dimensional datasets

our model also demonstrates excellent performance on non-high-dimensional data.

Visualization In Figure 5, we show the heatmap of the pair-wise column correlation of synthetic data and the real data. The colors in the image represent the absolute divergence between real and generated data, with lighter colors indicating smaller differences. It can be observed that the differences are significantly reduced, especially when comparing the baseline model of TabSyn to CtrTab, where the differences are noticeably minimized. This demonstrates that our proposed control module plays a significant role in improving the diffusion model’s ability to fit the distribution of high-dimensional data.

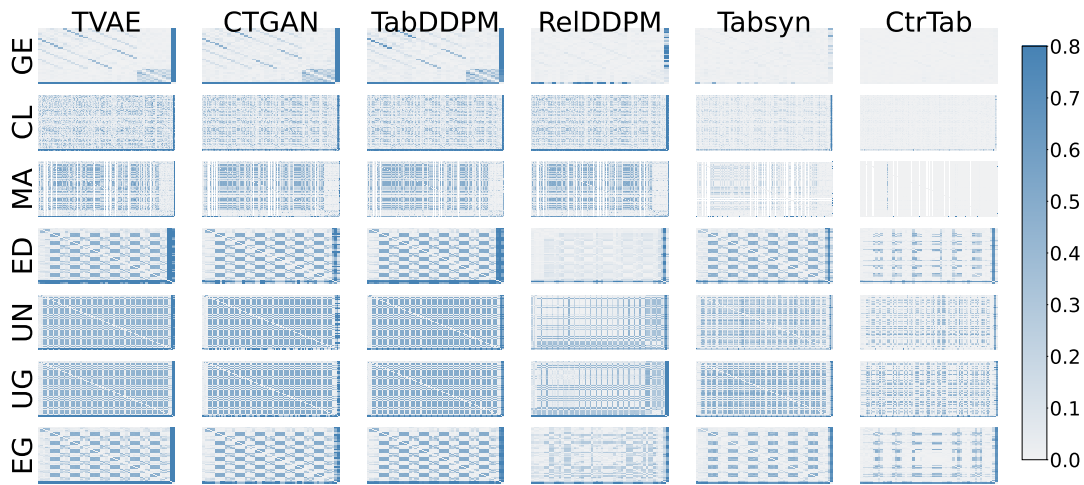


Figure 5: Heatmaps of the pair-wise column correlation of synthetic data v.s. the real data.

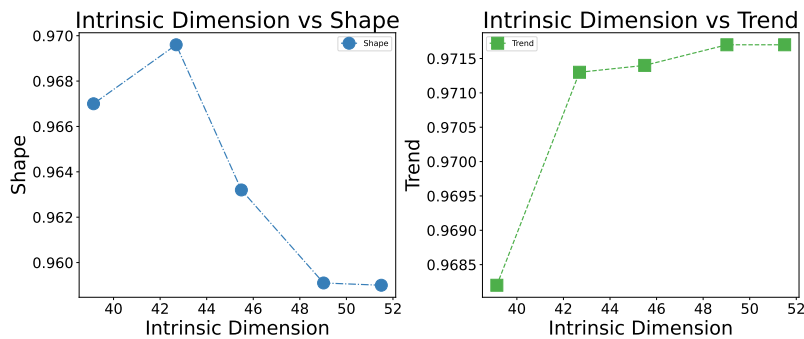


Figure 6: The impact of intrinsic dimensionality on generative performance

The impact of intrinsic dimensionality on generative performance. In this experiment, we explore the impact of different intrinsic dimensionalities of the data on the fitting performance of generative models.

We first use the method provided by sklearn to generate datasets with different intrinsic dimensions by controlling the strength of relationships between variables, while keeping the number of samples and dimensionality constant. Then, we train the TabSyn model and generate synthetic samples with the same number of training samples. Next, we evaluate the closeness between the generated data and real data from two perspectives: column-wise distribution and pair-wise column correlations.

For the column-wise distribution, since all datasets consist of numerical features, we use the Kolmogorov-Smirnov Test to measure the difference between the column-wise distributions of the generated and real data. For pair-wise column correlations, we use Pearson correlation to make comparisons. Figure 6 shows our results, where "Shape" represents the column-wise distribution and "Trend" represents the pair-wise column correlations.

It can be observed that, overall, as the intrinsic dimension increases, the "Trend" value increases while the "Shape" value decreases. This indicates that with higher intrinsic dimensions, the data structure becomes more complex, and the model's ability to fit pair-wise column correlations improves. However, as the data complexity increases, the model needs to learn more features and distribution details, resulting in a decrease in the "Shape" score. It is worth noting that the "Shape" value slightly increases at relatively low intrinsic dimensions. A possible explanation is that the data structure at this stage is relatively simple, making it easier for the model to fit the column-wise distribution. Nonetheless, the overall trend is a decrease in the "Shape" score.

Exploring the impact of different types of Noise on Model performance. In this experiment, we study whether adding different types of noise to the control input of our model affects the generated results. We compared the differences between adding Gaussian noise, uniform noise and the Laplacian noise used in our model. We compare the performance of different noise types by controlling the DCR value of the generated data. We also compared the ML performance of the model under these conditions. Table 8 presents our results, showing that Laplacian noise performs slightly better than other noise.

Datasets	Noise Type	F1↑	AUC↑	DCR↓
GE	Normal	0.604	0.876	0.995
	Laplace	0.618	0.881	0.994
	Uniform	0.613	0.879	0.996
CL	Normal	0.975	0.999	0.976
	Laplace	0.981	1.000	0.972
	Uniform	0.984	0.998	0.972
MA	Normal	0.995	0.999	0.180
	Laplace	0.994	0.999	0.178
	Uniform	0.995	0.999	0.181
ED	Normal	0.913	0.987	0.991
	Laplace	0.916	0.987	0.991
	Uniform	0.913	0.985	0.992
UN	Normal	0.894	0.976	0.998
	Laplace	0.896	0.979	0.999
	Uniform	0.890	0.978	0.999

Datasets	Noise Type	F2↑	RMSE↓	DCR↓
UG	Normal	0.985	0.092	0.993
	Laplace	0.988	0.084	0.992
	Uniform	0.934	0.181	0.993
EG	Normal	0.647	0.115	0.992
	Laplace	0.651	0.115	0.992
	Uniform	0.636	0.117	0.992

Table 8: Comparison of Normal noise, Laplace noise and Uniform noise on different datasets. Under the condition of maintaining similar (unnormalized) DCR values, we test the impact of the different types of noise on the generated results using the machine learning test.